

Bounds on Ratios of DIS Structure Functions from the Color Dipole Picture

Carlo Ewerz ^{a,1}, Otto Nachtmann ^{b,2}

^a ECT*, Strada delle Tabarelle 286, I-38050 Villazzano (Trento), Italy

^b Institut für Theoretische Physik, Universität Heidelberg
Philosophenweg 16, D-69120 Heidelberg, Germany

Abstract

We derive bounds on ratios of deep inelastic nucleon structure functions from the color dipole picture of high energy photon-hadron scattering. We find an upper bound on the ratio $R = \sigma_L/\sigma_T$ of the total cross sections for longitudinally and transversely polarized photons. We further obtain bounds on the ratio of deep inelastic structure functions F_2 taken at the same energy but at different photon virtualities. It is shown that these bounds can be used to constrain the range of applicability of the dipole picture.

¹ email: Ewerz@ect.it

² email: O.Nachtmann@thphys.uni-heidelberg.de

1 Introduction

The precise determination of the proton structure function F_2 in deep inelastic scattering (DIS) at high energy has been a major achievement of the H1 and ZEUS experiments at the HERA collider [1, 2, 3, 4, 5]. Much attention has been given to the region of small Bjorken- x where F_2 exhibits a significant growth as x decreases. This kinematical region is very interesting since here one can study the properties of a very dense system of partons. At ever smaller values of x or with increasing energy the parton densities should become so large that parton recombination processes are significant. It is expected that then a saturation of parton densities takes place, eventually taming the further rise of F_2 [6, 7, 8]. To date it is still an open question whether the energy available at HERA is already sufficiently high to probe this interesting and so far unexplored regime of QCD.

The smallest values of x accessible at HERA occur for relatively small photon virtualities Q^2 , thus prohibiting the use of perturbative QCD. In addition, also the high parton densities in this region make the theoretical description rather involved. In order to study possible saturation effects one therefore has to use theoretical models which do or do not incorporate saturation effects and to compare them with the experimental data. A prominent example of a saturation model is the Golec-Biernat-Wüsthoff model [9, 10]. The most widely used framework for implementing such models is the color dipole picture of high energy scattering [11, 12, 13]. The dipole picture is motivated by perturbation theory and describes photon-proton scattering as a two-step process. In the first step the photon splits into a quark-antiquark pair – the color dipole. In the second step this quark-antiquark pair scatters off the proton in the forward direction. While the dipole picture is certainly accurate at large photon virtualities and asymptotically large energy, the situation is less clear at moderate or low Q^2 , and for presently available energies. To obtain the dipole picture from a genuinely nonperturbative description of photon-proton scattering requires a number of approximations and assumptions [14, 15]. It is intrinsically difficult to determine their accuracy and to estimate the size of potential corrections to the dipole picture. Therefore it is important to constrain the range of applicability of the dipole picture before one can use it to draw conclusions about saturation, for example.

In this Letter we present bounds on ratios of structure functions from the dipole picture. These bounds are derived only from the general formulae constituting the dipole picture and are independent of any particular model for the dipole-proton scattering process. Any violation of these bounds by the experimental data would indicate a breakdown of the dipole picture. We show that in this way our bounds can indeed be used to constrain the range of applicability of the dipole picture.

2 The Dipole Picture

The amplitude for the splitting of a transversely (T) or longitudinally (L) polarized photon into a quark-antiquark pair of given flavor q in a high energy photon-hadron scattering process is given by the so-called photon wave function $\psi_{T,L}^{(q)}$. It depends on the photon virtuality Q^2 and on the quantum numbers specifying the color dipole, which are its size and orientation in the transverse space of the scattering process described by a two-dimensional vector \mathbf{r} , its longitudinal momentum \mathbf{q} in a given reference frame, the momentum fractions α and $(1-\alpha)$ of \mathbf{q} carried by the quark and antiquark, respectively, and finally the spin orientations of the quark and antiquark. In the following we will always sum over these spin orientations. The square of the photon wave function is obtained in leading order in the coupling constants α_{em} and α_s as

$$\left| \psi_T^{(q)}(\alpha, \mathbf{r}, Q) \right|^2 = \frac{3}{2\pi^2} \alpha_{\text{em}} Q_q^2 \{ [\alpha^2 + (1-\alpha)^2] \epsilon_q^2 [K_1(\epsilon_q r)]^2 + m_q^2 [K_0(\epsilon_q r)]^2 \} \quad (1)$$

and

$$\left| \psi_L^{(q)}(\alpha, \mathbf{r}, Q) \right|^2 = \frac{6}{\pi^2} \alpha_{\text{em}} Q_q^2 Q^2 [\alpha(1-\alpha)]^2 [K_0(\epsilon_q r)]^2 \quad (2)$$

for transversely and longitudinally polarized photons, respectively. Here $r = \sqrt{\mathbf{r}^2}$, Q_q are the quark charges in units of the proton charge, and K_0 and K_1 are modified Bessel functions. The quantity $\epsilon_q = \sqrt{\alpha(1-\alpha)Q^2 + m_q^2}$ involves the quark mass m_q . We then define a density for the photon wave function by integrating over the longitudinal momentum fraction α ,

$$w_{T,L}^{(q)}(r, Q^2) = \int_0^1 d\alpha \left| \psi_{T,L}^{(q)}(\alpha, \mathbf{r}, Q) \right|^2. \quad (3)$$

It describes the probability that a photon of virtuality Q^2 splits into a color dipole of size r and flavor q .

The second step of the photon-proton scattering process in the dipole picture is then the scattering of the dipole of size r off the proton, given by the so-called dipole cross section $\hat{\sigma}^{(q)}$. It depends on the dipole size r and on the squared center-of-mass energy W^2 in the dipole-proton system. Accordingly, the cross section for the photon-proton scattering process is then obtained by folding the photon density with the dipole-proton cross section, and by summing over all quark flavors q ,

$$\sigma_{T,L}(W^2, Q^2) = \sum_q \int d^2r w_{T,L}^{(q)}(r, Q^2) \hat{\sigma}^{(q)}(r, W^2). \quad (4)$$

The integration is over all dipole sizes and orientations. For a detailed discussion of the dipole picture, its nonperturbative foundations and potential correction terms see [14, 15].

Note that the energy variable in the dipole cross section is W^2 . In practical applications of the dipole picture one frequently uses Bjorken's $x = Q^2/(W^2 + Q^2 - m_p^2)$ instead. Strictly speaking, this is incorrect, since Q^2 is not uniquely determined by the properties of the dipole. The use of x is motivated by the fact that the photon densities $w_{T,L}$ are behaved in such a way that the integral in (4) is dominated by values of r around $4/Q^2$. Concentrating on the dominant values of r one can therefore trade W^2 for x . For a more detailed discussion of this point see [15]. We further note that in the limit of asymptotically high energy W the quark and antiquark forming the dipole are on their mass shell. In the dipole picture one therefore regards the dipole-proton scattering as a physical process. As such its cross section $\hat{\sigma}^{(q)}$ has to be non-negative.

Finally, we have for the structure function F_2 for $x \ll 1$ and $W^2 \gg m_p^2$

$$F_2(W^2, Q^2) = \frac{Q^2}{4\pi^2\alpha_{em}} [\sigma_T(W^2, Q^2) + \sigma_L(W^2, Q^2)] , \quad (5)$$

and the two terms in this sum are the transverse and longitudinal structure functions F_T and F_L , respectively.

3 Bound on $R = \sigma_L/\sigma_T$

We first consider the ratio of the cross sections for longitudinally and transversely polarized photons, $R(W^2, Q^2) = \sigma_L(W^2, Q^2)/\sigma_T(W^2, Q^2)$, or, equivalently, $R = F_L/F_T$. Recalling that σ_L and σ_T in (4) involve the same factor $\hat{\sigma}^{(q)}$, and that this factor as well as the photon densities $w_{T,L}^{(q)}$ of (3) are non-negative, it is straightforward to obtain upper and lower bounds on R in the dipole picture, valid for all W^2 ,

$$\min_{q,r} \frac{w_L^{(q)}(r, Q^2)}{w_T^{(q)}(r, Q^2)} \leq R(W^2, Q^2) \leq \max_{q,r} \frac{w_L^{(q)}(r, Q^2)}{w_T^{(q)}(r, Q^2)} . \quad (6)$$

Here the minimum and maximum are taken over all dipole sizes and over all quark flavors. Note that this bound is independent of the choice of energy variable (W^2 or x) in the dipole cross section. To prove (6) we start from the obvious inequalities

$$\min_{q,r} \frac{w_L^{(q)}(r, Q^2)}{w_T^{(q)}(r, Q^2)} \leq \frac{w_L^{(q)}(r, Q^2)}{w_T^{(q)}(r, Q^2)} \leq \max_{q,r} \frac{w_L^{(q)}(r, Q^2)}{w_T^{(q)}(r, Q^2)} . \quad (7)$$

Multiplying by the nonnegative factor $\hat{\sigma}^{(q)}w_T^{(q)}$, integrating over r and summing over q leads to inequalities equivalent to (6).

Using the explicit formulae (1) and (2) we find that the lower bound is trivial ($R \geq 0$). The most conservative upper bound, valid for all W^2 and Q^2 , is obtained by assuming the light quarks (u, d, s) to be massless, leading to the numerical value

$$R(W^2, Q^2) \leq 0.37248 . \quad (8)$$

Similarly, we can consider the cross sections $\sigma_{L/T}^{(q)}$ for heavy flavor production, $q = c, b$, which are naturally obtained via the flavor decomposition of (4). For the ratio $R_q = \sigma_L^{(q)}/\sigma_T^{(q)}$ we derive the bounds

$$\min_r \frac{w_L^{(q)}(r, Q^2)}{w_T^{(q)}(r, Q^2)} \leq R_q(W^2, Q^2) \leq \max_r \frac{w_L^{(q)}(r, Q^2)}{w_T^{(q)}(r, Q^2)}, \quad (9)$$

valid for all W^2 . The lower bound on R_c and R_b is again trivial, while the upper bound becomes Q^2 -dependent for heavy quarks. This dependence is shown in Fig. 1 together

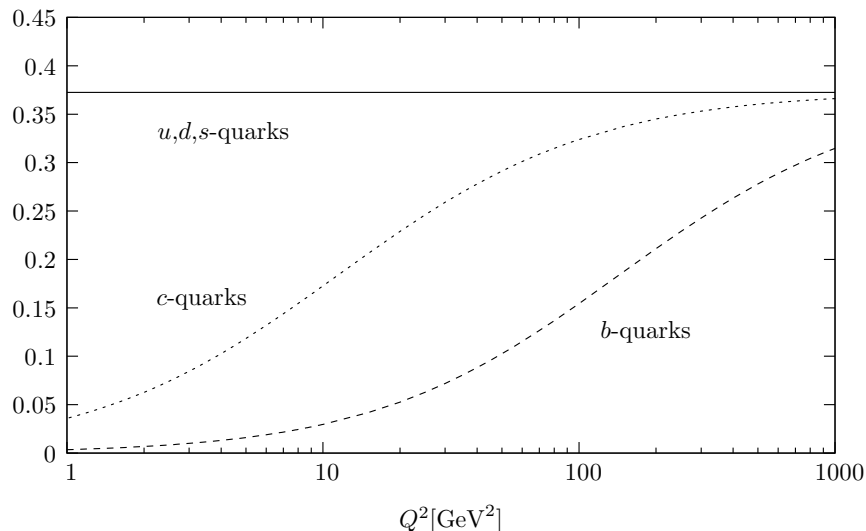


Figure 1: The upper bound on $R = \sigma_L/\sigma_T$ resulting from the dipole picture as a function of Q^2 . The solid line is for light quarks and constitutes the bound (6), (8). The lower lines are upper bounds on R_c and R_b , respectively, see (9).

with the bound (8) on R . Here we have used $m_c = 1.3 \text{ GeV}$ and $m_b = 4.6 \text{ GeV}$.

We now confront the bound (8) with the available experimental data on R at high energies which have been obtained by the NMC [16], CCFR [17], E143 [18], EMC [19] and CDHSW [20] collaborations. The scattering processes used to extract those data include not only $e^\pm p$ scattering but also other processes, among them muon and neutrino scattering on nuclear targets. In some of these processes one might in general expect additional caveats concerning the applicability of the dipole picture. For lack of further experimental data we nevertheless include the corresponding data points here. In order to have sufficiently high energy we restrict ourselves to data points with $x < 0.05$. Fig. 2 shows the available data together with the bound (8), where the few data points at $x < 0.01$ are represented by full points and those with $0.01 < x < 0.05$ as open points.

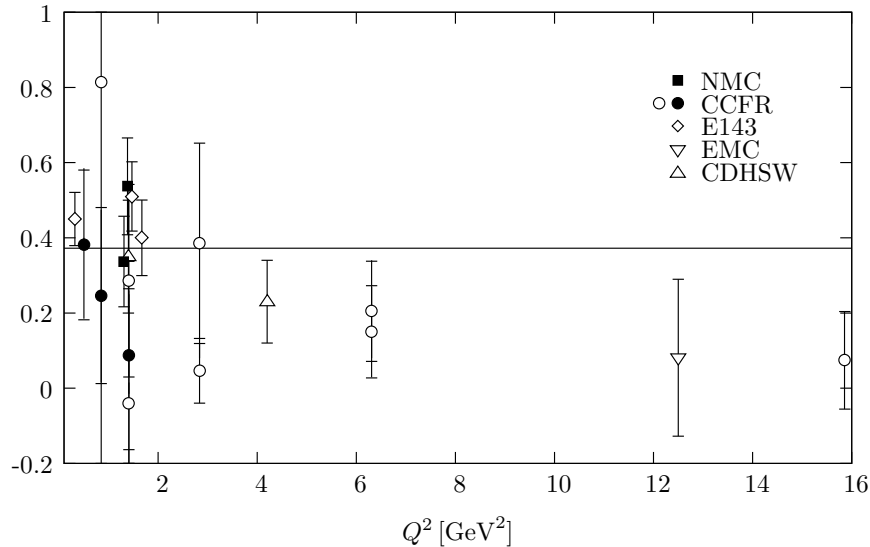


Figure 2: Comparison of experimental data for $R = \sigma_L/\sigma_T$ in the region $x < 0.05$ with the bound (8) resulting from the dipole picture. Full points correspond to data with $x < 0.01$, open points are data with $0.01 < x \leq 0.05$.

The data have large errors, but by and large they respect the bound. For Q^2 below about 2 GeV^2 , however, there seems to be the tendency that the data come close to the bound. Note the interesting fact that data very close to the bound could be accommodated in the dipole picture only if the dipole cross section $\hat{\sigma}^{(q)}$ were strongly peaked in r around the maximum of $w_L^{(q)}/w_T^{(q)}$ – which would appear to be very unlikely. Hence already data close to the bound can be interpreted as an indication of the breakdown of the dipole picture. In view of this we should be careful in interpreting the data at low Q^2 in terms of the dipole picture only. But the error bars of the presently available data on R are clearly too large to draw firm conclusions about the range of applicability of the dipole picture at low Q^2 .

So far, no direct measurements of F_L and R have been done at HERA. A discussion of the available indirect determinations of F_L in view of our bounds will be given elsewhere. Planned direct measurements of F_L at HERA will hopefully lead to a better determination of R , allowing for a stringent test of the validity of the dipole picture at low Q^2 .

A more detailed discussion of the bound on R is presented in the longer publication [15], where we also discuss diffractive scattering and give examples for the behavior of R in a typical saturation model.

4 Bounds on $F_2(W^2, Q_1^2)/F_2(W^2, Q_2^2)$

Next we turn to the ratio of structure functions F_2 taken at the same energy W but at different Q^2 , for which we can derive bounds in a way similar to those on R . We recall that the dipole cross section $\hat{\sigma}^{(q)}$ depends on r and W^2 , and is independent of Q^2 . (Note that this would not be the case if the energy variable in $\hat{\sigma}^{(q)}$ were x .) Therefore the cross sections of (4) and hence also F_2 involve the same factor $\hat{\sigma}^{(q)}(r, W^2)$ when evaluated at different Q^2 . Then the non-negativity of the photon densities $w_{T,L}^{(q)}$ and of the dipole cross section $\hat{\sigma}^{(q)}$ implies for all W^2 the bounds

$$\frac{Q_1^2}{Q_2^2} \min_{q,r} \frac{w_T^{(q)}(r, Q_1^2) + w_L^{(q)}(r, Q_1^2)}{w_T^{(q)}(r, Q_2^2) + w_L^{(q)}(r, Q_2^2)} \leq \frac{F_2(W^2, Q_1^2)}{F_2(W^2, Q_2^2)} \leq \frac{Q_1^2}{Q_2^2} \max_{q,r} \frac{w_T^{(q)}(r, Q_1^2) + w_L^{(q)}(r, Q_1^2)}{w_T^{(q)}(r, Q_2^2) + w_L^{(q)}(r, Q_2^2)}. \quad (10)$$

Also here, the most conservative bounds result from assuming the light quarks to be massless. They are shown in Fig. 3 for the choice $Q_2^2 = 10 \text{ GeV}^2$. The shaded region is

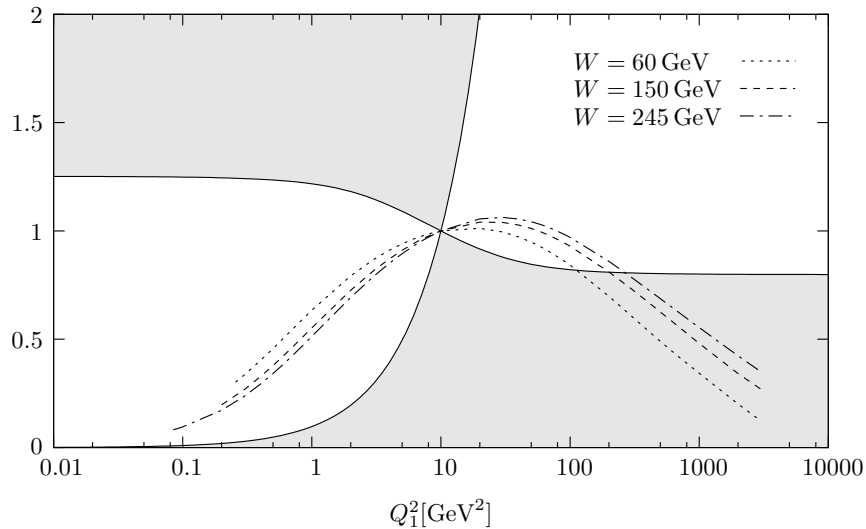


Figure 3: The bounds (10) on $F_2(W^2, Q_1^2)/F_2(W^2, Q_2^2)$ for $Q_2^2 = 10 \text{ GeV}^2$ and the corresponding fit to HERA data for three different values of W . Data in the shaded region cannot be described in the usual dipole picture.

excluded by the dipole picture.

Turning to the corresponding data we first note that the systematic errors in measurements of F_2 at different Q^2 are certainly not independent, making a determination of the error on the ratio somewhat involved. Here we only want to illustrate the consequences of the bound and leave a more sophisticated treatment of the errors as well

as the simultaneous variation of Q_1^2 and Q_2^2 for future work. We choose to compare the bound (10) with the so-called ALLM fit to F_2 [21, 22] which represents the data within their errors, with the possible exception of very low Q^2 where it underestimates the data of [1]. We further fix $Q_2^2 = 10 \text{ GeV}^2$ and consider only three energies $W = 60, 150, \text{ and } 245 \text{ GeV}$, roughly covering the kinematical range of HERA. For a given W we evaluate the ALLM fit only in the experimentally accessible Q^2 range. The Q_1^2 -dependence of the ratios of F_2 thus computed is confronted with the bounds in Fig. 3. The curves representing the data fall below the lower bound at values of Q_1^2 of about 100 to 200 GeV^2 , indicating a breakdown of the dipole picture. As expected, for larger W the corresponding curve remains within the bounds up to a higher Q_1^2 . The violation of the bound does not occur at a fixed x though. For the energies $W = 60, 150$ and 245 GeV the bound is violated at $x = 0.03, 0.008$ and 0.004 , respectively. At low Q_1^2 the ALLM fit does not come close to the bounds, hence its slight deviation from the data in this region is not relevant here.

Again, we can also derive separate bounds for the heavy flavor contribution $F_2^{q\bar{q}}$, $q = c, b$, to F_2 which is obtained from $\sigma_{T,L}^{(q)}$ in analogy to (5). These bounds then apply to $F_2^{q\bar{q}}(W^2, Q_1^2)/F_2^{q\bar{q}}(W^2, Q_2^2)$ and are of the same form as (10), but with the minimum and maximum taken only over r and not over q . We show them together with the

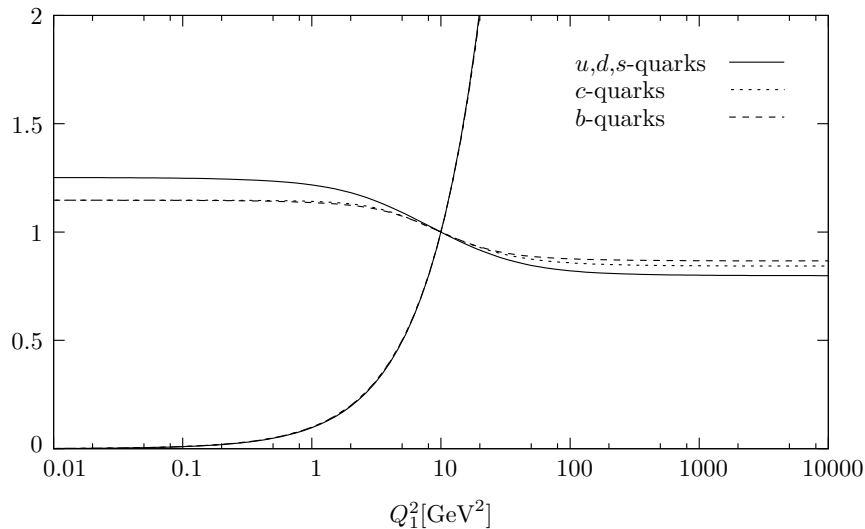


Figure 4: The bounds on $F_2^{q\bar{q}}(W^2, Q_1^2)/F_2^{q\bar{q}}(W^2, Q_2^2)$ for $q = c, b$ together with the bounds (10) (solid line) for $Q_2^2 = 10 \text{ GeV}^2$.

original bounds (10) in Fig. 4, again for $Q_2^2 = 10 \text{ GeV}^2$. For $Q_1^2 < Q_2^2$ the lower bound is insensitive to the quark mass, and the upper bound decreases with increasing quark mass. For $Q_1^2 > Q_2^2$, on the other hand, the upper bound is insensitive to the quark

mass, and the lower bound increases with increasing quark mass.

5 Summary

We have derived bounds on ratios of DIS nucleon structure functions from the usual color dipole picture. For this we have used the standard formulae for the photon wave functions and only the non-negativity of the dipole-nucleon cross sections. The bounds are hence independent of any model assumptions about the dipole-nucleon scattering. If a measurement of $R = \sigma_L/\sigma_T$ at given W^2 and Q^2 does not fulfill the bound (8) the dipole picture in the standard form is not valid there. If the ratio $F_2(W^2, Q_1^2)/F_2(W^2, Q_2^2)$ does not fulfill the bound (10) the dipole picture in the standard form is not valid at least at one of the two kinematical points. In all these cases correction terms to the standard dipole picture as discussed in [14, 15] must play a significant role, or the dipole picture may even break down completely.

In comparison with the data the bound on $R = \sigma_L/\sigma_T$ appears to suggest that we should be careful in interpreting the data at $Q^2 < 2 \text{ GeV}^2$ in terms of the dipole picture only. It is an interesting observation in this context that the possible evidence for saturation found by performing fits to the HERA data for F_2 in the dipole picture appears to depend on the inclusion of data at $Q^2 < 2 \text{ GeV}^2$ [23], that is exactly in the region in which the data on R come very close to the upper bound (8). For the bound on ratios of structure functions F_2 at the same W^2 but at different Q^2 the data constrain the use of the dipole picture for HERA energies to photon virtualities below around 100 to 200 GeV^2 . When analyzing HERA data in the framework of the dipole picture one should, therefore, restrict the analysis to the region allowed by these bounds in order to arrive at reliable conclusions.

Acknowledgements

We are grateful to J. Bartels, M. Klein, V. Lendermann, B. List, A. von Manteuffel, H. J. Pirner, and H.-C. Schultz-Coulon for helpful discussions. We thank A. Bodek and U. K. Yang for providing data for Fig. 2.

References

- [1] J. Breitweg *et al.* [ZEUS Collaboration], Phys. Lett. B **487**, 53(2000) [arXiv:hep-ex/0005018].
- [2] C. Adloff *et al.* [H1 Collaboration], Eur. Phys. J. C **21**, 33 (2001) [arXiv:hep-ex/0012053].

- [3] S. Chekanov *et al.* [ZEUS Collaboration], Eur. Phys. J. C **21**, 443 (2001) [arXiv:hep-ex/0105090].
- [4] C. Adloff *et al.* [H1 Collaboration], Eur. Phys. J. C **30**, 1 (2003) [arXiv:hep-ex/0304003].
- [5] S. Chekanov *et al.* [ZEUS Collaboration], Phys. Rev. D **70**, 052001 (2004) [arXiv:hep-ex/0401003].
- [6] L. V. Gribov, E. M. Levin and M. G. Ryskin, Phys. Rept. **100**, 1 (1983).
- [7] A. H. Mueller and J. Qiu, Nucl. Phys. B **268**, 427 (1986).
- [8] A. H. Mueller, Nucl. Phys. B **335**, 115 (1990).
- [9] K. Golec-Biernat and M. Wüsthoff, Phys. Rev. D **59**, 014017 (1999) [arXiv:hep-ph/9807513].
- [10] K. Golec-Biernat and M. Wüsthoff, Phys. Rev. D **60**, 114023 (1999) [arXiv:hep-ph/9903358].
- [11] N. N. Nikolaev and B. G. Zakharov, Z. Phys. C **49**, 607 (1991).
- [12] N. N. Nikolaev and B. G. Zakharov, Z. Phys. C **53**, 331 (1992).
- [13] A. H. Mueller, Nucl. Phys. B **415**, 373 (1994).
- [14] C. Ewerz and O. Nachtmann, arXiv:hep-ph/0404254.
- [15] C. Ewerz and O. Nachtmann, arXiv:hep-ph/0604087.
- [16] M. Arneodo *et al.* [New Muon Collaboration], Nucl. Phys. B **483**, 3 (1997) [arXiv:hep-ph/9610231].
- [17] U. K. Yang *et al.* [CCFR/NuTeV Collaboration], Phys. Rev. Lett. **87**, 251802 (2001) [arXiv:hep-ex/0104040].
- [18] K. Abe *et al.* [E143 Collaboration], Phys. Lett. B **452**, 194 (1999) [arXiv:hep-ex/9808028].
- [19] J. J. Aubert *et al.* [European Muon Collaboration], Nucl. Phys. B **259**, 189 (1985).
- [20] J. P. Berge *et al.*, Z. Phys. C **49**, 187 (1991).
- [21] H. Abramowicz, E. M. Levin, A. Levy and U. Maor, Phys. Lett. B **269**, 465 (1991).
- [22] H. Abramowicz and A. Levy, arXiv:hep-ph/9712415.
- [23] J. R. Forshaw and G. Shaw, JHEP **0412**, 052 (2004) [arXiv:hep-ph/0411337].